J. Astrophys. Astr. (1990) **11**, 193–208

Radiative Transfer With Compton Scattering in Plane Parallel Geometry

A. Peraiah *Indian Institute of Astrophysics, Bangalore 560034*

Received 1989 July 27; revised 1990 March 23; accepted 1990 April 5

Abstract. We have solved the equation of radiative transfer with Compton scattering. The specific intensity has been expanded by Taylor series with respect to wavelength and the first three terms have been retained in solving the transfer equation. It is noted that in a medium stratified in plane parallel layers, the multiple Compton scattering redistributes the initial energy over a range of 3 to 5 Compton wavelengths. A good fraction of the incident radiation is transferred across the layer with redistribution in wavelength, the actual value depending on the optical thickness of the medium.

Key words: radiative transfer—Compton scattering

1. Introduction

One of the many reasons for broadening and asymmetry of the spectral lines formed in the outer layers of stars is the scattering of radiation by free electrons which also contributes to the continuous opacity in hot stars. The electrons produce a change in wavelength of photons due to this effect. It is necessary to investigate how the energy is redistributed in wavelengths and what fraction of incident energy is emerging out of a plane parallel slab with consequent redistribution.

Pomraning & Froehlich (1969), considered the equation of transfer with Compton and inverse Compton scattering which admits an eigen-function expansion. Viik (1968a, b) attempted to solve the equation of transfer in an analytical way following Chandrasekhar's approach. However, no physical effects are shown. Missana & Piana (1976) have shown that Compton scattering can cause a reduction in the central intensity in the absorption and emission lines. Pozdnyakov, Sobol & Sunyaev (1976) have studied multiple Compton scattering of low frequency photons by relativistic electrons. Langer (1979) studied the problem of Comptonization of X-rays by cold-electrons by using Monte Carlo method. Nagel (1981) studied the problem of Comptonization in hot and strongly magnetized plasma using a two-stream transfer equation with redistribution of photons in a cyclotron line. Barbosa (1982) gives useful expressions for Compton scattering coefficients by evaluating the full Klein-Nishina cross-section. Missana (1982) suggested the possibility of a large Compton redshift in the spectra of β Orionis. Ipser & Price (1983) have shown that dissipative heating due to magnetic reconnection, and dissipation of turbulence leads to high accretion rates in a spherical accretion of gas onto a black hole, to densities and temperatures at

which Comptonization becomes important. Pozdynakov, Sobol & Sunyaev (1983) have described different aspects of Compton scattering. Czerny & Sztajno (1983) studied the effects of Compton scattering on the spectrum of X-ray bursts. You *et al.* (1982) studied the synchrotron self-Compton effect. Keiner & Shikhovtseva (1983) have obtained analytical solutions for the transfer equation for the photon density matrix in the case of inverse Compton reflection. Ochelkov & Usov (1983) analysed the spontaneous Compton scattering of electromagnetic radiation by ultra-elativistic particles in magnetic fields. Nagirner (1984) studied multiple Compton scattering by gas in which the photon energy is much less than the electron rest-energy. Gould (1984) has given the cross-section of double Compton scattering for $\gamma + r \gg e + \gamma + \gamma'$ for the energies in the spectrum of outgoing photons.

Sunyaev and Titarchuk (1985) considered Comptonization of low-frequency radiation in accretion discs. They have employed the method of successive approximations over the number of scatterings. However, they did not consider the frequency dependence of the scattering cross-section and indicatrix. They have shown that in the accretion discs the angular distribution and polarization of hard radiation forming via Comptonization, that is, multiple scatterings in the discs depend only on the optical thickness of the disc and are independent of either the photon frequency or the geometric distribution of low-frequency photons. They have presented calculations of polarization and angular distribution for several values of optical thickness. Bloemen (1985) studied the production of diffuse galactic gamma radiation above 1 MeV from the interaction of cosmic-ray electrons with the interstellar photon field. The source function for the inverse Compton scattering is described. Fukue, Kato & Matsumoto (1985) examined the radiative transfer in a hot moving plasma which interacts with photons through the Compton process. Xia *et al.* (1985) obtained the total cross-sections for the inverse Compton scattering in strong magnetic fields (10^{12}–10^{13} G). They found that these are large when the frequencies of the incoming photons are near the resonance frequencies. Guilbert (1986) obtained exact results for calculating Compton heating and cooling in optically thin gases. Kirk (1986) suggested that the flat spectrum of X-ray pulsars is due to the optically thin emission from resonant double Compton scattering. Bhat, Kifune & Wolfendale (1986) have used different data to determine the number of Cygnus X3 like X-ray sources in the Galaxy. They have developed a method of studying the number of sources which have existed in the past by way of high latitude inverse Compton photons. Lovelace (1987) developed a model for a possible early phase of extragalactic jets. Mezaros & Bussard (1986) calculated the angle-dependent Compton redistribution function which can be applied in studying X-ray sources. Daugherty & Harding (1986) calculated the angle-dependent Compton redistribution function which can be applied in studying X-ray sources. They also derived relativistic cross-sections for Compton scattering by electrons in strong magnetic fields. Zdziarski & Lamb (1986) presented a model of γ-ray burst sources based on repeated Compton scatterings of soft photons by relativistic nonthermal electrons. Nishimura, Mitsuda & Itoh (1986) studied analytically the Comptonization of soft X-ay photons in a plane parallel infinite plasma cloud. Kirk, Nagel & Storey (1986) solved the equation of transfer using Feautrier's method in calculating the phase dependent spectra of X-ray pulsars in a slab geometry,

Different methods of solution to the hard X-ray transfer problem are required. Particularly we need a method that works for soft and hard X-ray transfer problems

with Compton and inverse Compton scattering included. Peraiah (1986) has derived transmission and reflection functions with Compton scattering.

We start with the assumption that the medium is divided into plane parallel layers and each is of equal optical thickness. The scattered radiation is a function of the wavelength and therefore we have to consider the specific intensities in different wavelengths. For this purpose the specific intensity is expanded in Taylor series as was done in Chandrasekhar (1960) and Code (1967). However, these authors have considered only the first derivative $\partial I/\partial\lambda$ and we shall include the second derivative $\partial^2 I/\partial\lambda^2$ also so that the solution represents a fairly good approximation to the reality.

2. Calculations

Following Chandrasekhar (1960) and Code (1967), the equation of transfer can be written as,

$$\mu\frac{\partial I(z,\mu,\lambda)}{\partial z}=-KI(z,\mu,\lambda)+K\left[(1-\omega)B+\frac{\omega}{4\pi}\int_{-1}^{+1}\int_{0}^{2\pi}I(z,\mu',\lambda-\delta\lambda)d\mu'd\varphi'\right], \tag{1}$$

where

$$\delta\lambda=\gamma(1-\cos\theta), \tag{2}$$

$$\gamma=\frac{h}{mc}=0.024\ \text{Å}, \tag{3}$$

B = Planck function,

$$\cos\theta=\mu\mu'+(1-\mu^2)^{1/2}(1-\mu'^2)^{1/2}, \tag{4}$$

ω = albedo for single scattering.

We have to consider the contribution of $I(z,\ \mu',\lambda\ \delta\lambda\ )$ to the radiation field after scattering. We shall expand $I(z,\ \mu',\ \lambda-\delta\lambda)$ by Taylor series as,

$$I(z,\mu',\lambda-\delta\lambda)=I(z,\mu',\lambda)-\frac{\delta\lambda}{1!}\frac{\partial I(z,\mu',\lambda)}{\partial\lambda}+\frac{(\delta\lambda)^2}{2!}\frac{\partial^2 I(z,\mu',\lambda)}{\partial\lambda^2}. \tag{5}$$

After substituting equation (5), in (1) and performing the integration over φ' we obtain,

$$\mu\frac{\partial I(z,\mu,\lambda)}{\partial z}=-KI(z,\mu,\lambda)+K\left[(1-\omega)B+\frac{\omega}{2}\int\left\{I(z,\mu',\lambda)-\gamma(1-\mu\mu')\times\frac{\partial I(z,\mu',\lambda)}{\partial\lambda}+\left[\frac{1}{2}\gamma^2\left((1-\mu\mu')^2+\frac{1}{2}(1-\mu^2)(1-\mu'^2)\right)\times\frac{\partial^2 I(z,\mu',\lambda)}{\partial^2\lambda}\right]\right\}d\mu'\right]. \tag{6}$$

We shall retain the two terms containing $\partial I/\partial\lambda$ and $\partial^2 I/\partial\lambda^2$ and choose the points for wavelengths in steps of the Compton wavelength. If we choose n discrete points of λ,

then we have η equations each similar to that given in (6). Therefore we have *n* terms of $\partial I_i/\partial\lambda i$, and $\partial^2 I_i/\partial^2\lambda_i$ in *n* equations. The term $\partial Ii/\partial\lambda i$, is replaced by its difference as given below.

$$\frac{\partial I_i}{\partial\lambda_i}=\frac{I_i-I_{i-1}}{\lambda_i-\lambda_{i-1}}.$$

When all the *n* equations are considered, the quantities $\partial I_i/\partial\lambda_i$, $\partial I_{i+1}/\partial\lambda_{i+1}$, $\partial I_{i+2}/\partial\lambda_{i+2}$ *etc.* will form into a vector. Consequently the terms $\partial I/\partial\lambda$ in *n* equations when combined will form into $\mathbf{D_1I}$ where

$$\mathbf{D}_1=\begin{bmatrix} -\frac{1}{\lambda_2-\lambda_1} & \frac{1}{\lambda_2-\lambda_1} & & \\ -\frac{1}{\lambda_2-\lambda_1} & 0 & \frac{1}{\lambda_3-\lambda_1} & \\ & -\frac{1}{\lambda_4-\lambda_2} & 0 & \frac{1}{\lambda_4-\lambda_2} \\ & \ddots & \ddots & -\frac{1}{\lambda_n-\lambda_{n-1}} \end{bmatrix} \tag{7}$$

and

$$\mathbf{I}=[I_1, I_2, \ldots, I_n]^{\mathrm{T}}, \tag{8}$$

where λ's are the quadrature points (trapezoidal points here) and I_1, I_2 *etc.* are the corresponding intensities. Similarly the $\partial^2 I/\partial\lambda^2$ term can be written as $\mathbf{D_2I}$, where

$$\mathbf{D}_2=\begin{bmatrix} \frac{1}{(\Delta\lambda)^2} & -\frac{2}{(\Delta\lambda)^2} & \frac{1}{(\Delta\lambda)^2} & & \\ 0 & \frac{1}{(\Delta\lambda)^{2-}} & \frac{2}{(\Delta\lambda)^2} & \frac{1}{(\Delta\lambda)^2} & \\ & & \ddots & \ddots & \frac{1}{(\Delta\lambda)^2} \\ & & & & -\frac{1}{(\Delta\lambda)^2} \end{bmatrix} \tag{9}$$

and **I** is the corresponding intensity vector. We choose m angle points on Gauss-Legendre quadrature.

The transfer equation in (6) is integrated on the angle-wavelength mesh as described in Peraiah & Grant (1973; hereafter referred to as PG). After integration, we have

$$\begin{aligned}\mathbf{M}[\mathbf{I}^+_{n+1}-\mathbf{I}^+_n]+\tau_{n+1/2}\mathbf{I}^+_{n+1/2}=\tau_{n+1/2}(1-\omega)\mathbf{B}^+_{n+1/2}+(\tfrac{1}{2}\omega\mathbf{P}^{++}_{n+1/2}\mathbf{C}\\ -\gamma\mathbf{P}^{++}_{1,n+1/2}\mathbf{Cd}_{1,n+1/2}\\ +\tfrac{1}{2}\gamma^2\mathbf{P}^{++}_{2,n+1/2}\mathbf{Cd}_{2,n+1/2})\mathbf{I}^+_{n+1/2}\\ +(\tfrac{1}{2}\omega\mathbf{P}^{+-}_{n+1/2}\mathbf{C}-\gamma\mathbf{P}^{+-}_{1,n+1/2}\mathbf{Cd}_{1,n+1/2}\\ +\tfrac{1}{2}\gamma^2\mathbf{P}^{+-}_{2,n+1/2}\mathbf{Cd}_{2,n+1/2})\mathbf{I}^-_{n+1/2}.\end{aligned} \tag{10}$$

For the oppositely directed beam,

$$\begin{aligned}\mathbf{M}[\mathbf{I}_n^- - \mathbf{I}_{n+1}^-] + \tau_{n+1/2}\mathbf{I}_{n+1/2}^- = \tau_{n+1/2}(1-\omega)\mathbf{B}_{n+1/2}^- + (\tfrac{1}{2}\omega\mathbf{P}_{n+1/2}^{-+}\mathbf{C} \\ -\gamma\mathbf{P}_{1,n+1/2}^{-+}\mathbf{C}\mathbf{d}_{1,n+1/2} + \tfrac{1}{2}\gamma^2\mathbf{P}_{2,n+1/2}^{-+}\mathbf{C}\mathbf{d}_{2,n+1/2})\mathbf{I}_{n+1/2}^+ \\ +(\tfrac{1}{2}\omega\mathbf{P}_{n+1/2}^{--}\mathbf{C} - \gamma\mathbf{P}_{1,n+1/2}^{--}\mathbf{C}\mathbf{d}_{1,n+1/2} \\ +\tfrac{1}{2}\gamma^2\mathbf{P}_{2,n+1/2}^{--}\mathbf{C}\mathbf{d}_{2,n+1/2})\mathbf{I}_{n+1/2}^- . \end{aligned} \tag{11}$$

The quantities Q^{++}, Q^{--} *etc.* in PG will become

$$\mathbf{Q}_{n+1/2}^{++} = \tfrac{1}{2}\omega_{n+1/2}\mathbf{P}_{n+1/2}^{++}\mathbf{C} - \gamma\mathbf{P}_{1,n+1/2}^{++}\mathbf{C}\mathbf{d}_1 + \tfrac{1}{2}\gamma^2\mathbf{P}_{2,n+1/2}^{++}\mathbf{C}\mathbf{d}_{2,n+1/2}, \tag{12}$$

$$\mathbf{Q}_{n+1/2}^{--} = \tfrac{1}{2}\omega_{n+1/2}\mathbf{P}_{n+1/2}^{--}\mathbf{C} - \gamma\mathbf{P}_{1,n+1/2}^{--}\mathbf{C}\mathbf{d}_1 + \tfrac{1}{2}\gamma^2\mathbf{P}_{2,n+1/2}^{--}\mathbf{C}\mathbf{d}_{2,n+1/2}, \tag{13}$$

$$\mathbf{Q}_{n+1/2}^{-+} = \tfrac{1}{2}\omega_{n+1/2}\mathbf{P}_{n+1/2}^{-+}\mathbf{C} - \gamma\mathbf{P}_{1,n+1/2}^{-+}\mathbf{C}\mathbf{d}_1 + \tfrac{1}{2}\gamma^2\mathbf{P}_{2,n+1/2}^{-+}\mathbf{C}\mathbf{d}_{2,n+1/2}, \tag{14}$$

$$\mathbf{Q}_{n+1/2}^{+-} = \tfrac{1}{2}\omega_{n+1/2}\mathbf{P}_{n+1/2}^{+-}\mathbf{C} - \gamma\mathbf{P}_{1,n+1/2}^{+-}\mathbf{C}\mathbf{d}_1 + \tfrac{1}{2}\gamma^2\mathbf{P}_{2,n+1/2}^{+-}\mathbf{C}\mathbf{d}_{2,n+1/2}, \tag{15}$$

where

$$\mathbf{P}^{++} = \begin{bmatrix} \mathbf{p}^{++} & & \\ & \mathbf{p}^{++} & \\ & & \ddots \end{bmatrix} = \mathbf{P}^{+-} = \mathbf{P}^{-+} = \mathbf{P}^{--}, \tag{16}$$

$$P^{++}(\mu_j, \mu_k) = 1, \tag{17}$$

$$P_1^{++} = \begin{bmatrix} P_1^{++} & & \\ & P_1^{++} & \\ & & \ddots \end{bmatrix}, \tag{18}$$

$$P_1^{++}(j,k) = \{1 - (+\mu_j)(+\mu_k)\}, \tag{19}$$

$$P_1^{++} = \begin{bmatrix} P_1^{+-} & & \\ & P_1^{+-} & \\ & & \ddots \end{bmatrix}, \tag{20}$$

with

$$P_1^{+-}(j,k) = \{1 - (+\mu_j)(-\mu_k)\}. \tag{21}$$

Similarly P_1^{-+}, P_1^{--} and P_1^{-+} and P_1^{--} are defined.

$$\mathbf{M} = \begin{bmatrix} \mathbf{m} & & \\ & \mathbf{m} & \\ & & \ddots \end{bmatrix}, \mathbf{m} = [\mu_{jk}, \delta_{jk}], \tag{22}$$

$$\mathbf{C} = \begin{bmatrix} \mathbf{C} & & \\ & \mathbf{C} & \\ & & \ddots \end{bmatrix}, \mathbf{C} = [C_{jk}, \delta_{jk}]. \tag{23}$$

The quantities s^{++}, s^{--}, s^{+-}, s^{-+} in Peraiah & Grant (1973) become

$$\mathbf{S}^{++}_{n+1/2} = \mathbf{M} - \tfrac{1}{2}\tau_{n+1/2}\mathbf{E} + \tfrac{1}{4}\tau_{n+1/2}\omega_{n+1/2}\mathbf{P}_{n+1/2}\mathbf{C} - \tfrac{1}{2}\tau_{n+1/2}\gamma\mathbf{P}^{++}_{1,n+1/2}\mathbf{Cd}_{1,n+1/2} + \tfrac{1}{4}\tau_{n+1/2}\gamma^2\mathbf{P}^{++}_{2,n+1/2}\mathbf{Cd}_{2,n+1/2}, \tag{24}$$

$$\mathbf{S}^{--}_{n+1/2} = \mathbf{M} - \tfrac{1}{2}\tau_{n+1/2}\mathbf{E} + \tfrac{1}{4}\tau_{n+1/2}\gamma^2\omega_{n+1/2}\mathbf{P}^{--}_{n+1/2}\mathbf{C} - \tfrac{1}{2}\tau_{n+1/2}\gamma\mathbf{P}^{--}_{1,n+1/2}\mathbf{Cd}_{1,n+1/2} + \tfrac{1}{4}\tau_{n+1/2}\gamma^2\mathbf{P}^{--}_{2,n+1/2}\gamma^2\mathbf{Cd}_{2,n+1/2}, \tag{25}$$

$$\mathbf{S}^{-+}_{n+1/2} = \tfrac{1}{4}\tau_{n+1/2}\omega_{n+1/2}\mathbf{P}^{-+}_{n+1/2}\mathbf{C} - \tfrac{1}{2}\tau_{n+1/2}\gamma\mathbf{P}^{-+}_{1,n+1/2}\mathbf{Cd}_1 + \tfrac{1}{4}\tau_{n+1/2}\gamma^2\mathbf{P}^{-+}_{2,n+1/2}\mathbf{C}_2\mathbf{d}_{2,n+1/2}, \tag{26}$$

$$\mathbf{S}^{+-}_{n+1/2} = \tfrac{1}{4}\tau_{n+1/2}\omega_{n+1/2}\mathbf{P}^{+-}_{n+1/2}\mathbf{C} - \tfrac{1}{2}\tau_{n+1/2}\gamma\mathbf{P}^{+-}_{1,n+1/2}\mathbf{Cd}_{1,n+1/2} + \tfrac{1}{4}\tau_{n+1/2}\gamma^2\mathbf{P}^{-+}_{1,n+1/2}\mathbf{Cd}_{2,n+1/2}, \tag{27}$$

and

$$(\Delta^+)^{-1}_{n+1/2} = \mathbf{M} + \tfrac{1}{2}\tau_{n+1/2}\mathbf{E} - \tfrac{1}{4}\tau_{n+1/2}\omega_{n+1/2}\mathbf{P}^{++}_{n+1/2}\mathbf{C} + \tfrac{1}{2}\tau_{n+1/2}\gamma\mathbf{P}^{++}_{1,n+1/2}\mathbf{Cd}_{1,n+1/2} - \tfrac{1}{4}\tau_{n+1/2}\gamma^2\mathbf{P}^{++}_{2,n+1/2}\mathbf{Cd}_{2,n+1/2}, \tag{28}$$

$$(\Delta^-)^{-1}_{n+1/2} = \mathbf{M} + \tfrac{1}{2}\tau_{n+1/2}\mathbf{E} - \tfrac{1}{4}\tau_{n+1/2}\omega_{n+1/2}\mathbf{P}^{--}_{n+1/2}\mathbf{C} + \tfrac{1}{2}\tau_{n+1/2}\gamma\mathbf{P}^{--}_{1,n+1/2}\mathbf{Cd}_{1,n+1/2} - \tfrac{1}{4}\tau_{n+1/2}\gamma^2\mathbf{P}^{--}_{2,n+1/2}\mathbf{Cd}_{2,n+1/2}, \tag{29}$$

where $\tau_{n+1/2}$ is the mean optical depth of the nth layer and E is the unit matrix. The transmission and reflection operators follow those given in PG.

3. Results and discussion

The radiation field is calculated according to the procedure described in PG. We have considered 3 different cases of total optical depths: T = 1.0, 2.0 and 5.0. The medium is

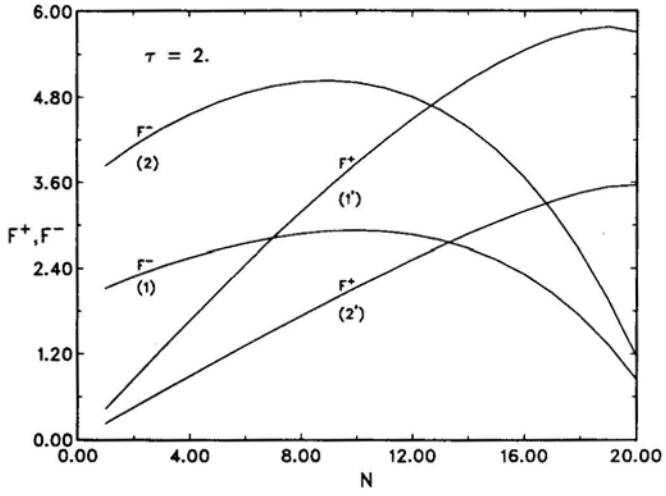

Figure 1. The inward (F^+) and outward (F^-) fluxes are plotted against the shell numbers. Curves 1 and 1′ represents the fluxes without the $\partial^2 I/\partial\lambda^2$ term and curves 2 and 2′ represent the curves calculated by including the $\partial^2 I/\partial\lambda^2$ term.

divided into 20 plane parallel layers each of equal optical thickness. We have considered 4 angle points and 10 frequency points. The wavelength points are chosen in units of Compton wavelength γ. Trapezoidal points are choosen for frequency mesh and are taken as $\gamma, 2\gamma, \ldots, 10\gamma$, so that the step length is one Compton wavelength. The roots and weights of Gauss-Legendre quadrature on $\mu \in (0, 1)$ are chosen as the angle points. We have chosen 4 angle points μ_1, μ_2, μ_3 and μ_4 on $\mu \in (0,1)$ with the corresponding weights C_1, C_2, C_3 and C_4 (Abramowicz & Stegun 1965) given by

$$\begin{aligned} \mu_1 &= 0.06943, & C_1 &= 0.17393, \\ \mu_2 &= 0.33001, & C_2 &= 0.32607, \\ \mu_3 &= 0.66999, & C_3 &= 0.32607, \\ \mu_4 &= 0.93057, & C_4 &= 0.17393. \end{aligned}$$

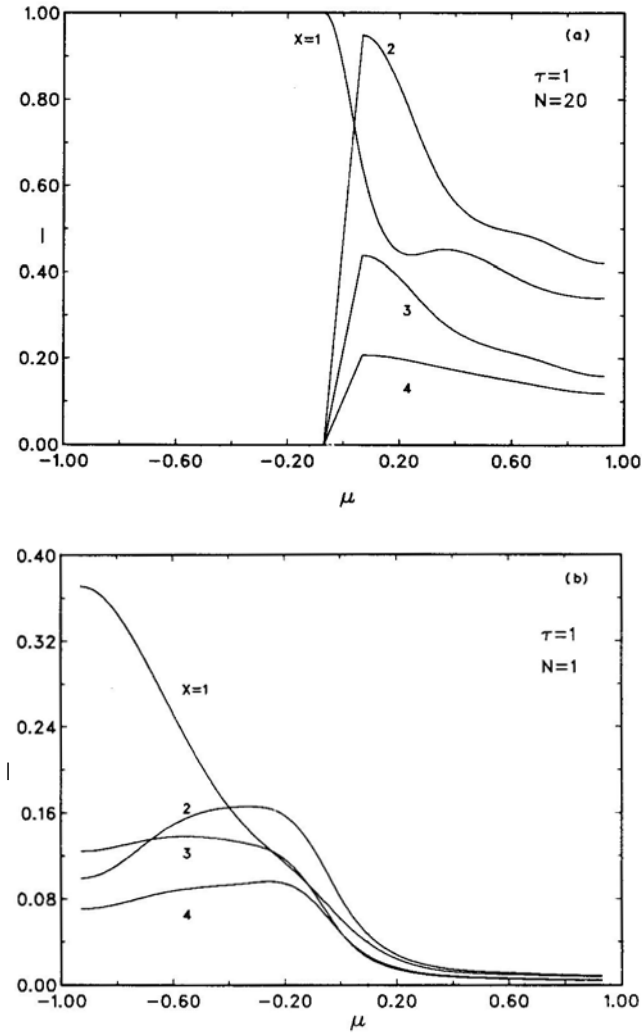

Figure 2. (a) Angular distribution of specific intensities at $\tau = T = 1 (N = 20)$, and (b) the emergent intensities at $\tau = 0$.

We have given incident radiation at $\tau = T$ and no radiation is incident at $\tau = 0$:

$$I^-(\mu_j, x(1), \tau = T) = 1.0,$$
$$I^-(\mu_j, x(2, \ldots 10), \tau = T) = 0,$$
$$I^+(\mu_j, x_i, \tau = 0) = 0.$$

In Fig. 1, we presented a comparison of the calculations performed with and without the term $\partial^2 I/\partial\lambda^2$. Here N represents the number of layers. $N = 20$ represents the layer where $\tau = \tau_{\max} = T$ and $N = 1$ represents the layer where $\tau = 0$, the emergent side of the medium. We calculated the inward and outward fluxes F^+ and F^- for a total optical depth of 2.0. The inward fluxes (F^+) in both the cases (for 1′ and 2′ in Fig.

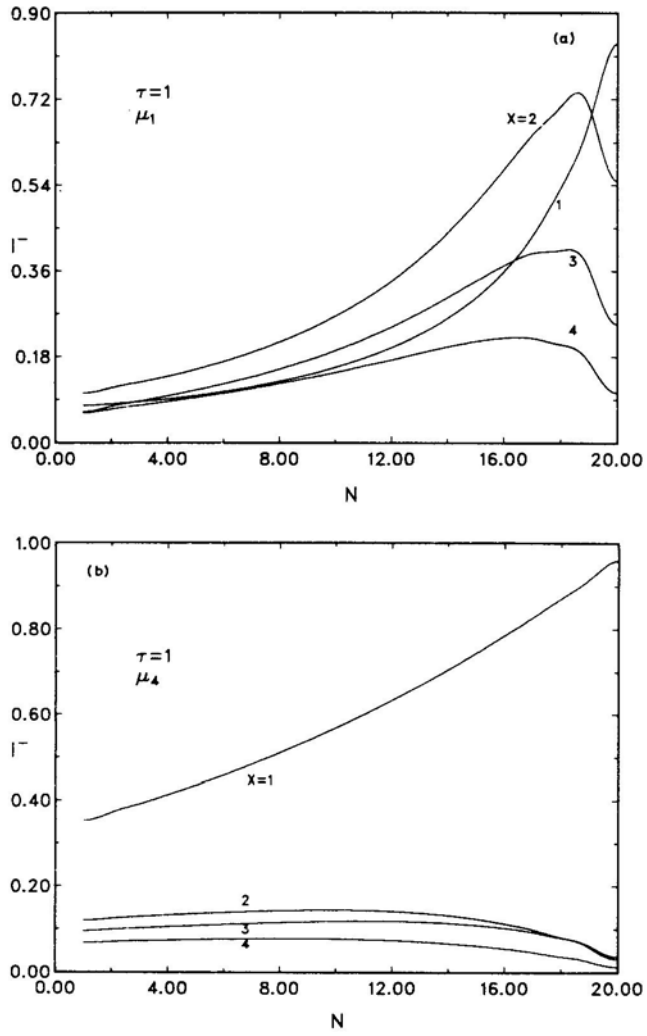

Figure 3. The emergent intensities across the medium corresponds to different Compton wavelengths (x) and for the angular (a) μ_1 and (b) μ_4. Here $N = 1$ corresponds to the emergent intensities and at $N = 20$ corresponds to $\tau = T$.

1) are larger at $N = 20$ or $\tau = T$ because of the back scattering at the innermost surface. The contribution to this comes from the diffuse radiation field from the layer bounded by $\tau = 0$ and $\tau = T$. However the effect of back scattering is reduced considerably towards the emergent side of the layer and only a small fraction of the flux is directed towards the surface $\tau = T$. The emergent fluxes (F^-) in both cases behave in a different way. Although these fluxes are considerably smaller than those of (F^+) they reach maxima at about $N = 10$ exactly halfway of the layer and then fall slowly towards the emergent side of the shell ($\tau = 0$). We can see that the introduction of the term $\partial^2 I/\partial\lambda^2$ into the calculations produces considerable changes in the radiation field. It also shows that we cannot compare these results with those of Chandrasekhar (1960).

In Figs 2(a) and (b) we show the angular distribution of specific intensities for a total optical depth $T = 1$. Unit intensity at $x = \gamma$ is incident at $\tau = T$. We see in Fig. 2(a), that

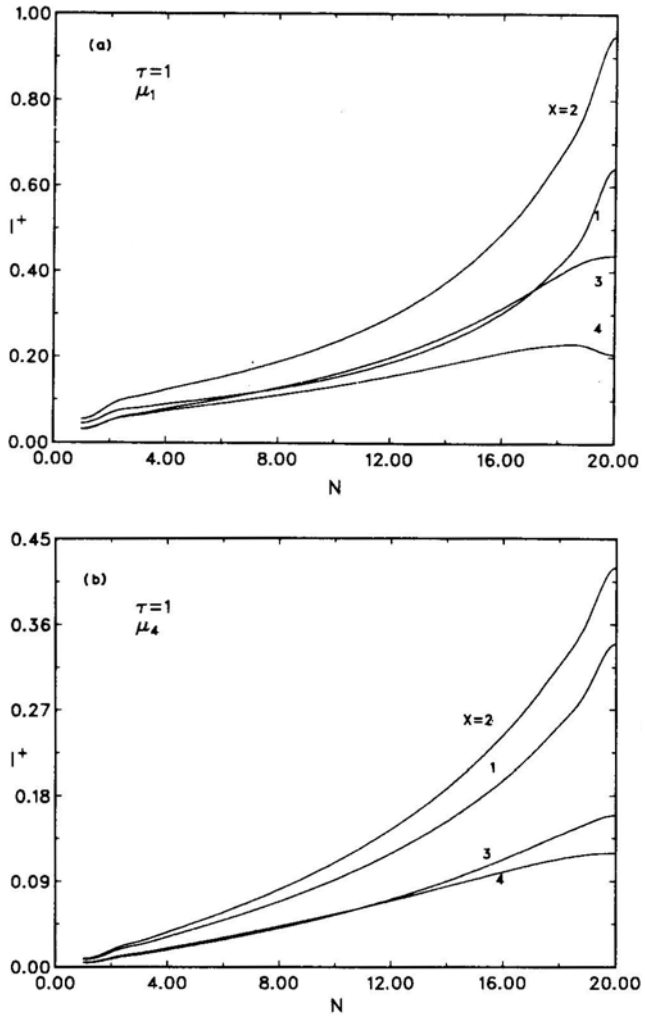

Figure 4. The redistribution of intensities across the medium for the inward scattered specific intensities corresponding to (a) μ_1 and (b) μ_4.

the outward intensities are all equal to 1 unit at $x = \gamma$ for all μ_j and no radiation is directed outwards $[-1 < \mu < 0]$ at wavelength $x = 2\gamma, 3\gamma, 4\gamma$. We also notice that a small amount of radiation is directed into the medium $[0 < \mu < 1]$ at wavelengths $x = \gamma, 2\gamma, 3\gamma$ and 4γ. It is interesting that more radiation is scattered at $x = 2\gamma$ instead of at $x = \gamma$. The radiation at $x = 3\gamma$ and 4γ is a small fraction of that at $x = \gamma$ in the range of $-1 \leqslant \mu < 0$. This is expected because of the diffuse radiation field contributed by the medium between $\tau = 0$ and $\tau = T$.

In Fig. 2(b), the angular distribution of radiation field is presented at the shell $N = 1$ or $\tau = 0$ which is the emerging side of the medium. Most of the radiation is directed outwards while in Fig. 2(a) in which the radiation is shown at $N = 20$ ($\tau = T$) we see

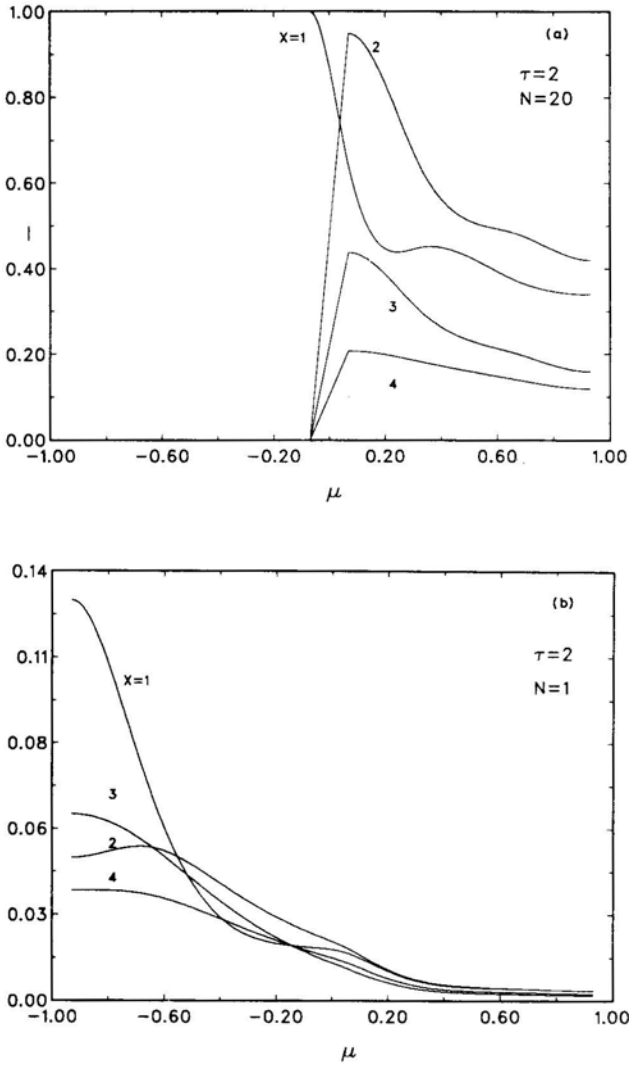

Figure 5. (a) Angular distribution of specific intensities at $\tau = T = 2$, and (b) the emergent intensities at $\tau = 0$.

that the trend is opposite to what is seen in Fig. 2(b). Largest fraction of radiation is transferred through the specific intensity at $x = 1$. The radiation in the range $0 < \mu \leqslant 1$ (backward directed radiation) is considerably small.

It would be interesting to see how the radiation is redistributed across the medium corresponding to different directions and wavelengths after several Compton scatterings. In Figs 3(a) and (b) we plot the distribution of radiation directed towards the emergent side across the medium for the directions μ_1 and μ_4 respectively for different values of x (we have not plotted values for $x > 4\gamma$ because these values are small). In the direction μ_1, we see that a substantial part of radiation is emergent for $x = \gamma$ and the radiation corresponding to $x = \gamma$, 3γ and 4γ is slightly less than that at x

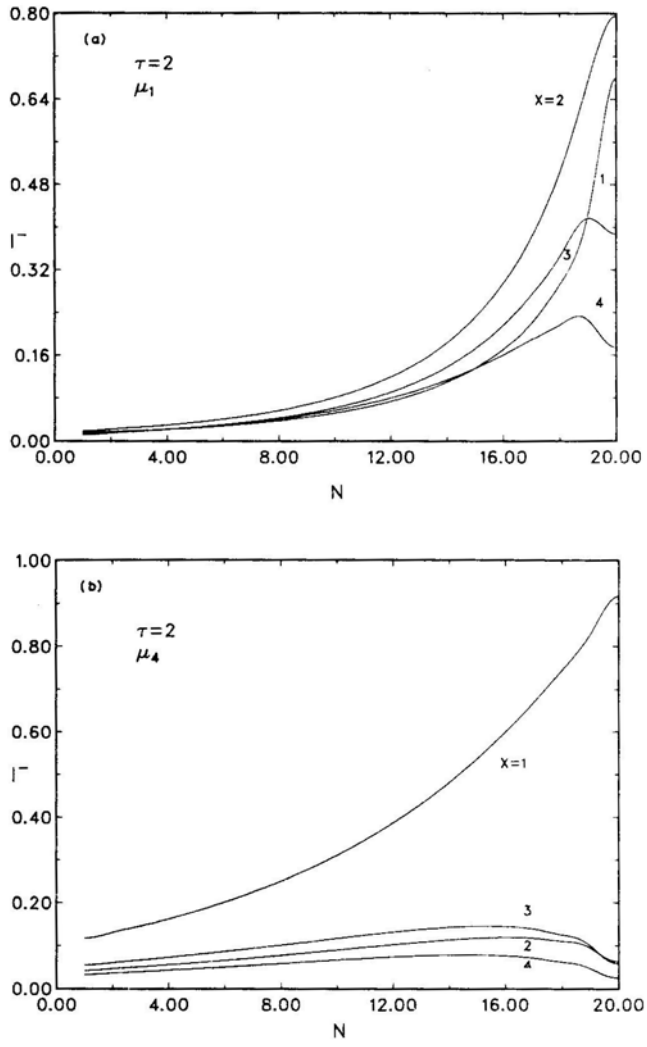

Figure 6. The emergent intensities across the medium corresponding to different Compton wavelengths and for the direction (a) μ_1 and (b) μ_4. Here $N = 1$ corresponds to the emergent intensities and $N = 20$ corresponds to $\tau = T$.

$= 2\gamma$. In the direction μ_4 most of the radiation is emerging in the wavelength $x = \gamma$ while the emergent radiation at $x = 2\gamma$, 3γ and 4γ is about 25 per cent of that at $x = \gamma$. The rays corresponding to μ_4 and μ_1 carry more energies at $x = \gamma$ and $x = 2\gamma$. In Fig. 4(a) and (b), we plot the inward directed intensities across the medium for the directions μ_1 and μ_4 respectively. It appears that the maximum intensities occur at $N = 20$ and at $N = 1$ ($\tau = 0$). Very little radiation is directed into the medium. More radiation is redistributed in the wavelength $x = 2\gamma$ than in other wavelengths, *i.e.,* $x = \gamma$, 3γ and 4γ in both the directions μ_1 and μ_4. This is slightly different from the radiation directed outwards (see Figs 3(a) and (b)).

In Fig. 5(a), we present the angular distribution of the intensities for $\tau = 2$ at $N = 20$. The variation of I is similar to that shown in Fig. 2(a). In Fig. 5(b), we plot the angular

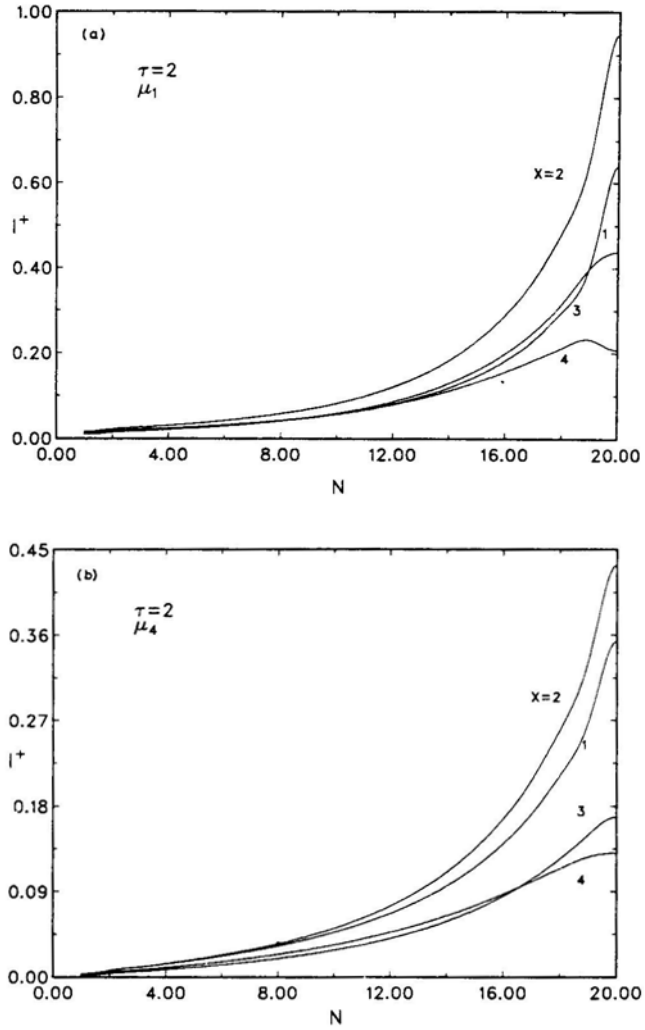

Figure 7. The redistribution of radiation across the medium for the inward scattered specific intensities corresponding to (a) μ_1 and (b) μ_4.

distribution of I at $N = 1$ or $\tau = 0$. Major fraction of radiation is distributed at $x = \gamma$, and the intensities at $x = 2\gamma$, 3γ and 4γ are quite small. If we compare these results with those presented in Fig. 2(b), we notice that the magnitudes of the intensities given in Fig. 5(b) are reduced considerably. This is due to higher optical depth used in the latter calculations. The backward directed radiation ($0 < \mu \leqslant 1$) is negligibly small.

In Figs 6(a) and (b) we plot the redistribution of the radiation across the medium. Larger fraction of radiation is redistributed at the wavelength $x = 2\gamma$ which is similar to the distribution shown in Figs 3 and 2(b). Figs 7(a) and (b) describe the distribution of intensities across the medium for $\tau = 2$ in the directions μ_1 and μ_4 respectively. They show the same behaviour as in Figs 4(a) and (b).

Fig. 8(a) gives the angular distribution at $N = 20$ or $\tau = 5$. Although the optical depth is higher than what is used to calculate the results given in Figs 2(a) and 5(a), we

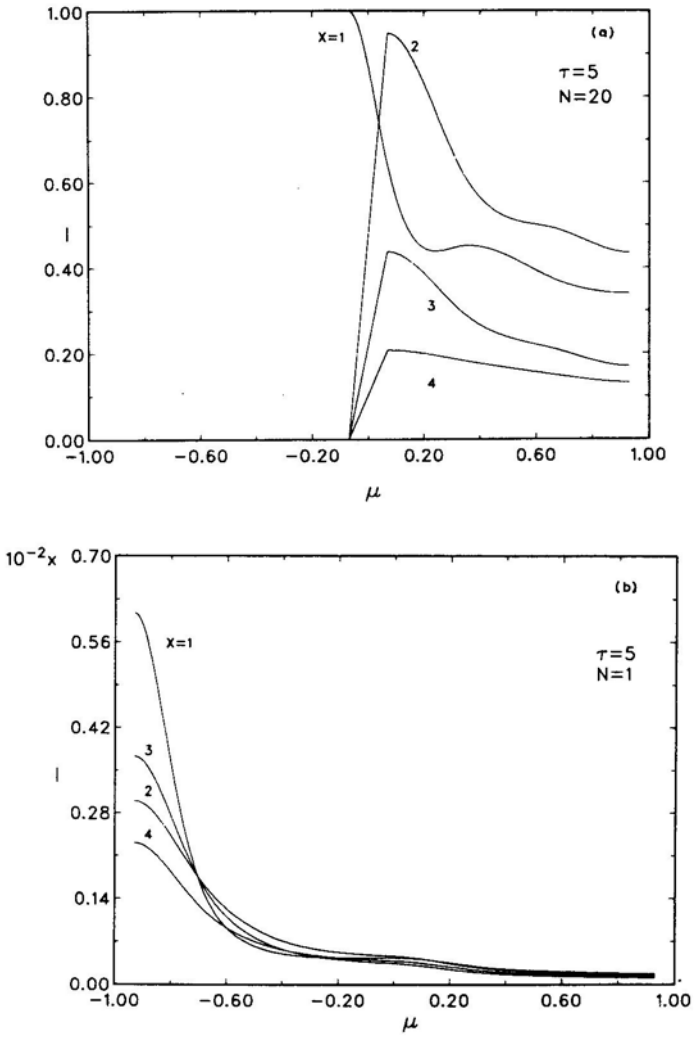

Figure 8. (a) Angular distribution of specific intensities at $\tau = T = 5$, and (b) the emergent intensities at $\tau = 0$.

find the behaviour at $\tau = 5$. In Fig. 8(b), the angular distribution of the emergent intensities is described. The magnitudes of intensities is considerably reduced due to the larger optical depth. Moreover, we see that radiation is spread to $x = 3\gamma$ more than at $x = 2\gamma$ near $\mu \approx -1$. Figs 9(a) and (b) describe the distribution of outward directed radiation across the medium at $x = \gamma$, 2γ, 3γ and 4γ in the direction μ_1. However the radiation in the direction μ_4 is emerging mostly at wavelengths $x = \gamma$ and 3γ.

The backward directed intensities in the direction μ_1 and μ_2 are plotted in Figs 10(a) and (b). The trend is the same as that shown in Figs 7(a) and (b); that is, more back-scattered radiation is in wavelength $x = 2\gamma$.

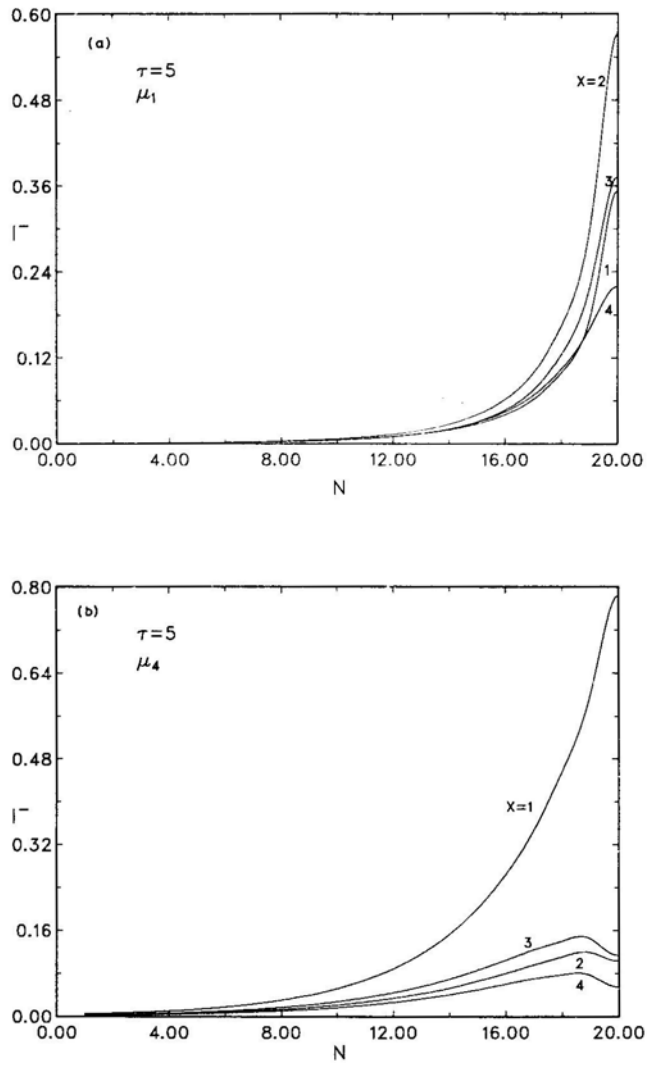

Figure 9. The emergent intensities across the medium corresponding to different Compton wavelengths and for the angular (a) μ_1 and (b) μ_2. Here $N = 1$ corresponds to the emergent intensities and $N = 20$ corresponds to $\tau = \tau_{max}$.

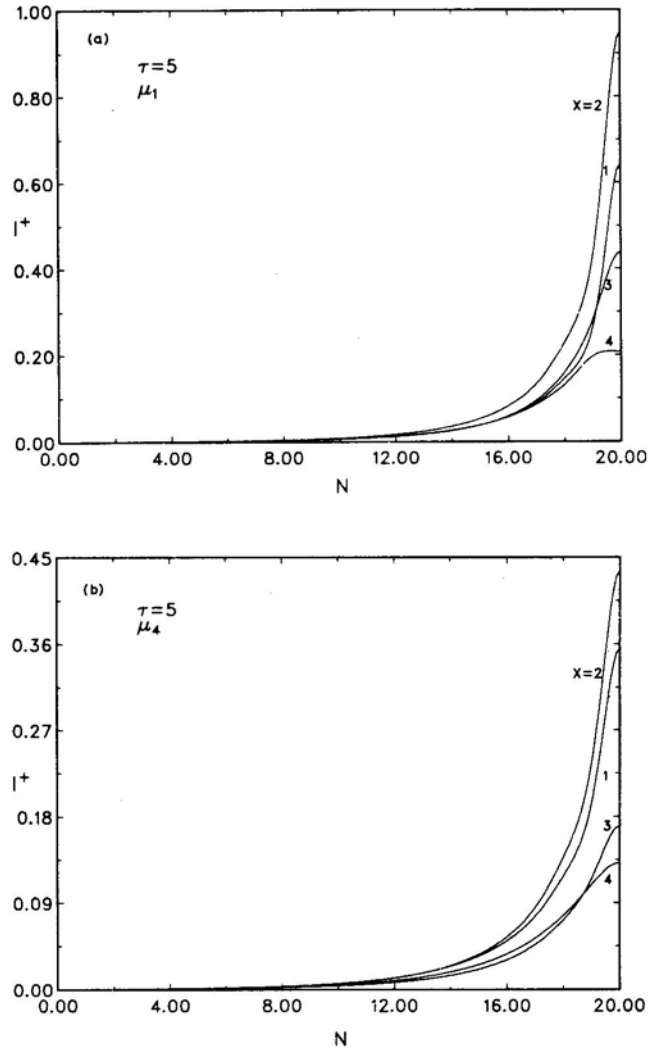

Figure 10. The redistribution of radiation across the medium for the involved scattered specific intensities corresponding to (a) μ_1 and (b) μ_4.

References

Abramowicz, M., Stegun, I. A. 1972, *Hand book of Mathematical Functions,* Dover, New York.
Barbosa, D. D. 1982, *Astrophys. J.,* **254**, 301.
Bhat, C. L, Kifune, T., Wolfendale, A. W. 1986, *Astr. Astrophys.,* **159**, 299.
Bloemen, J. B. G. M.1985, *Astr. Astrophys.,* **145***,* 391.
Chandrasekhar, S. 1960, *Radiative Transfer,* Dover, New York.
Code, A. D. 1967, *Astrophys. J.,* **149**, 253.
Czerny, M., Sztajno, M. 1983, *Acta Astronomica,* **33**, 213.
Daugherty, J. K. Harding, A. K. 1986, *Astrophys. J.* **309**, 362.
Fukue, J., Kato S., Matsumoto R. 1985, *Publ. astr. Soc. Japan,* **37**, 383.
Gould, R. J. 1984, *Astrophys. J.,* **285**, 275.
Guilbert, P. W. 1986, *Mon. Not. R. astr. Soc,* **218**, 171.

Ipser, J. R., Price, R. H. 1983, *Astrophys. J.,* **267**, 371.
Keiner, S. R., Shikhovtseva, E. S. 1983, *Astrophysics,* **19**, No. 4.
Kirk, J. G. 1986, *Astr. Astrophys.,* **158**, 305.
Kirk, J. G., Nagel, W., Storey, M. C. 1986, *Astr. Astrophys.,* **169**, 259.
Langer, S. H. 1979, Astrophys. J, **232**, 891.
Lovelace, R. V. E. 1987, *Astr. Astrophys.,* **173**, 237.
Meszaros, P., Bussard R. W. 1986, *Astrophys. J.,* **306**, 238.
Missana, M. 1982, *Astrophys. Sp. Sci.,* **85**, 137.
Missana, M., Piana A. 1976, *Astrophys. Sp. Sci.,* **43**, 129.
Nagel, W. 1981, *Astrophys. J.,* **251**, 288.
Nagirner, D. I. 1984, *Astrophysics,* **20**, 95.
Nishimura, J., Mitsuda, K., Itoh, M. 1986, *Publ. astr. Soc. Japan,* **38**, 819.
Ochelkov, Yu. P., Usov, V. V. 1983, *Astrophy. Sp. Sci.,* **96**, 55.
Peraiah, A. 1986, *Kodaikanal. Obs. Bull,* **5**, 113.
Peraiah, A., Grant, I. P. 1973, *J. Inst. Maths, Appl,* **12**, 75 (PG).
Pomraning, G. C, Froehlich, R. 1969, *Astr. Astrophys.,* **1**, 286.
Pozdnyakov, L. A., Sobol, I. M., Sunyaev, R. A. 1976, *Sov. Astr.,* **2**, L55.
Pozdnyakov, L. A., Sobol, I. M., Sunyaev, R. A. 1983, *Astrophys. Sp. Phys. Rev.,* **2**, 189.
Strong, A. W. 1985, *Astr. Astrophys.,* **145**, 81.
Sunyaev, R. A., Titarchuk, L. G. 1985, *Astr. Astrophys.,* **143**, 374.
Viik, T. 1968a, *Tartu Astr. Obs. Teated,* No. 19, p. 71.
Viik, T. 1968b, *Tartu Astr. Obs. Teated,* No. 19, p. 91.
Xia, X. Y., Qiao, G. J., Wu, X. J., Hou Y. Q. 1985, *Astr. Astrophys.,* **152**, 93.
You, J. -h., Xie, G.-z., Bao, M.-x., Li K.-h. 1982, *Acta Astr. Sinica,* **23**, 353.
Zdziarski, A. A., Lamb, D. Q. 1986, *Astrophys. J.,* **309**, L362.